

Effect of TiC and Mo₂C on Hydrogen Desorption of Mechanically Milled MgH₂

Mi Tian¹, Congxiao Shang^{2*}

School of Environmental Sciences, University of East Anglia,

Norwich, NR4 7TJ, UK

¹mtian@uea.ac.uk, ^{2*}c.shang@uea.ac.uk

Abstract- Titanium carbide (TiC) and molybdenum carbide (Mo₂C) particles were selected to modify the hydrogen storage properties of magnesium hydride (MgH₂). (MgH₂+ 2 mol% TiC) and (MgH₂+2 mol% Mo₂C) mixtures were prepared using both cryogenic milling and high-energy ball milling. The morphology and crystallite structure of the mixtures were examined by X-ray diffraction (XRD), scanning electron microscopy (SEM) and transmission electron microscopy (TEM). The milled (MgH₂+TiC) and (MgH₂+Mo₂C) composites consisted of γ -MgH₂ and β -MgH₂. TiC nanoparticles with the size of 10~20 nm after milling were deposited onto the surface or into the grain boundary of MgH₂. Mo₂C were uniformly distributed on the surface of MgH₂ particles. Thermogravimetry and derivative thermogravimetric analyses showed that ~6.5 wt. % hydrogen was desorbed from (MgH₂+TiC) mixture in the temperature range from 190 to 400 °C at a heating rate of 10 °C/min under He flow. The on-set and peak temperatures were 190 and 280 °C, respectively, for (MgH₂+TiC) ball-milled up to 60 hrs after 8 hrs cryomilling. However, (MgH₂+Mo₂C) shows much higher desorption temperature of 300 °C (on-set) and 358 °C (peak), respectively, compared with those recorded for (MgH₂+TiC). The hydrogen desorption activation energy of the milled (MgH₂+TiC) mixture, 104 kJ/mol, was also substantially reduced, compared with that of the (MgH₂+ Mo₂C) mixture, 167 kJ/mol. The addition of TiC nanoparticles has greater effect on reduction of hydrogen desorption temperatures and acceleration of desorption kinetics.

Keywords- Hydrogen Storage; MgH₂; TiC; Mo₂C; Nanoparticles; Mechanical Milling; Cryogenic Milling

I. INTRODUCTION

Magnesium hydride has been considered one of promising hydrogen storage materials due to its high hydrogen capacity of 7.6 wt %, high abundance, low cost and light weight [1, 2]. However its slow kinetics and high desorption temperature (>300 °C) limit its practical applications. Many methods, such as doping with catalysts, reducing crystallinity and particle size, have been developed to improve the hydrogen desorption properties. According to recent studies, the desorption kinetics and temperatures of MgH₂ have been dramatically improved by ball milling with some transition metals, oxides and carbides [3-6]. Transition-metal compounds attracted considerable interest as effective catalysts, due to the high affinity of transition-metal cation toward hydrogen [2]. Titanium compounds have been successfully used to improve the sorption kinetics in several typical hydrogen storage systems, exhibiting a high affinity toward hydrogen even at moderate temperatures. For example, titanium halides are exceptionally effective in lowering the kinetic barrier of dehydrogenation reactions for alkaline alanates [7-9]. Recently, it has been found that the temperature for hydrogen release from MgH₂ can be greatly reduced by doping it with Ti-containing agents [10, 11]. In addition, it was reported that graphite as a codopant

of titanium-based catalyst enhanced significantly both the hydrogenation and the dehydrogenation kinetics of catalyzed MgH₂ and NaAlH₄ [11, 12]. Comparative studies based on various transition-metal oxides emphasize that an appropriate chemical interaction between catalyst and host hydride is essential for realizing high catalytic activity [13]. The interactions between the hydrides and the transition metal agents weaken the Mg-H bonds and thus facilitate the recombination of hydrogen atoms to the hydrogen molecules.

TiC has been found to be an effective and stable catalyst for hydrogen desorption of MgH₂ in our recent work [4]. However, the effect of other transition metal carbides on the hydrogen sorption of MgH₂ has not been well studied previously. Here, a systematic investigation was carried out on the hydrogen desorption properties of MgH₂ catalyzed by a small amount of TiC or Mo₂C. The effects of TiC and Mo₂C were compared. Both cryogenic milling and high-energy ball milling were used to reduce the hydrogen desorption temperatures and kinetics of MgH₂.

II. EXPERIMENTAL METHODS

As-received MgH₂ powder (from Th. Goldschmidt AG, Degussa, ~95 % MgH₂, 5 % Mg, 50 μ m) was mixed with 2 mol. % of TiC powder (from Sigma-Aldrich, ~95 wt. %, < 200 nm) or 2 mol. % of Mo₂C powder (from Sigma-Aldrich, 99.5%, < 44 μ m). The mixtures were cryogenically milled for 8 hrs using liquid nitrogen to freeze the sealed milling vial in a SPEX SamplePrep 6750 Freezer/Mill, then mechanically milled for 16 hrs and 60 hrs at ambient temperature using a high energy ball mill, SPEX 8000D, under Argon atmosphere. The initial ball-to-powder weight ratio is 10:1. All the powder handling was performed in a dry glove box under high purity argon.

The morphology of the powder mixtures was characterized by a Jeol 6300 scanning electron microscopy (SEM). The powder particle sizes were calculated from the SEM pictures as the equivalent circle diameter, $ECD = (4A/\pi)^{1/2}$, where A represents the projected particle area, using the *Image Tool v.3.00* software. A Jeol 1010 transmission electron microscopy (TEM) was used for further examination of the nano-structures of the mixtures. X-ray diffraction (XRD) was performed using an XTra diffractometer, manufactured by Thermo ARL (US), with Cu K α radiation. The crystallite/gain sizes were calculated from XRD data using Scherrer equation [14].

The hydrogen sorption behavior of the mixtures was studied by Intelligent Gravimetric Analysis (IGA, Hidden Isochem Ltd.). The desorption was performed from 20 to 500 °C under 1 bar helium pressure with a heating rate of 10 °C/min and He flow rate of 150 ml/min.

III. RESULTS AND DISCUSSION

A Structure Characterization

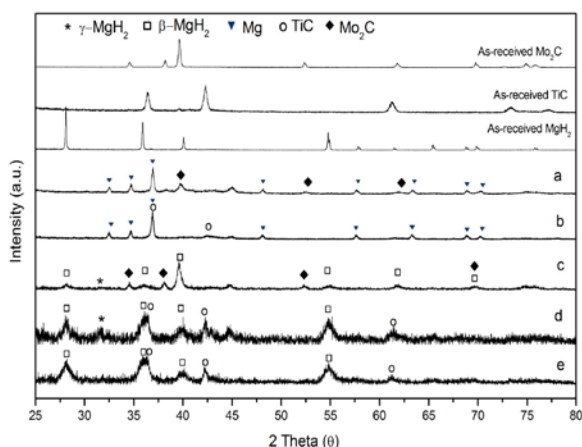


Fig.1 X-ray diffraction patterns of the as-received MgH_2 , TiC , Mo_2C , the milled (MgH_2+TiC) and ($\text{MgH}_2+\text{Mo}_2\text{C}$) mixtures. (a) Dehydrogenated ($\text{MgH}_2+\text{Mo}_2\text{C}$) after cryomilling and 60 hrs ball milling, (b) Dehydrogenated (MgH_2+TiC) after cryomilling and 60 hrs ball milling, (c) 60 hrs ball-milled ($\text{MgH}_2+\text{Mo}_2\text{C}$) after cryomilling, (d) 60 hrs ball-milled (MgH_2+TiC) after cryomilling, (e) 8 hrs cryomilled (MgH_2+TiC)

Fig. 1 presents XRD patterns of the (MgH_2+TiC) and ($\text{MgH}_2+\text{Mo}_2\text{C}$) mixtures cryomilled for 8 hrs and further ball-milled for 60 hours. After cryogenic and ball milling processes, the main phases presented are the parent materials, MgH_2 , TiC or Mo_2C . There were no new compounds formed from the mixtures. The metastable orthorhombic $\gamma\text{-MgH}_2$ is detected concurrently with $\beta\text{-MgH}_2$ in 60 hrs ball-milled (MgH_2+TiC) and ($\text{MgH}_2+\text{Mo}_2\text{C}$) after 8 hrs pre-cryomilling. The formation of $\gamma\text{-MgH}_2$ during high energy ball milling of MgH_2 has been reported previously [15]. The $\gamma\text{-MgH}_2$ is a high-pressure polymorphic form of $\beta\text{-MgH}_2$ created due to the localized on-contact impacting action of steel balls on the MgH_2 powder particles in the milling vial [16, 17]. It is suggested that the formation of $\gamma\text{-MgH}_2$, as a metastable high-pressure phase, has a positive effect on hydrogen desorption process as a result of rearrangement in the cation and anion substructures, destabilizing $\beta\text{-MgH}_2$ and reduce the desorption temperature [16-18]. From XRD pattern of the dehydrogenated (MgH_2+TiC) mixture cryomilled for 8 hrs and further ball-milled for 60 hrs, only MgH_2 and TiC peaks are detected in the dehydrogenated mixtures. There is no reaction between TiC and Mg/MgH_2 . Similarly, Mo_2C retains its original form during milling and after dehydrogenation. Both TiC and Mo_2C are stable compounds with formation enthalpies of -190.4 ± 17.0 kJ/mol [19] and -107.35 kJ/mole [20] respectively. The XRD peaks of MgH_2 become broadened with increase of milling time, indicating the decrease of crystallite size, compared with the as-received powders.

Fig. 2 shows estimates of the grain size of as-received MgH_2 calculated from XRD patterns [14] to be of the order of 65 nm. After 8 hrs cryogenic milling, the grain size of MgH_2 has decreased greatly to ~ 25 nm. It has been suggested that the presence of liquid nitrogen during cryomilling has several advantages, such as decreased oxygen contamination [21] and enhanced deformation during milling [22]. Following a further 60 hrs ball milling, the grain size of MgH_2 was only reduced slightly to 20 nm. This indicates that the cryogenic milling process is very effective in reducing the grain size of MgH_2

particles and further high energy ball milling only reduces the grain size to a minor extent. Cryogenic milling provides significant improvement to surface residual stresses and the effectiveness of grinding forces. This is due to substantial temperature reduction within grinding zone and a decrease in the magnitude of tensile residual stress for all the materials [23]. Cryogenic milling offers an effective solution for achieving fine powders by enhancing the brittleness of the materials and reducing their tensile strength for materials [22]. The grain size of TiC does not decrease greatly after 8 hrs cryomilling (~ 17 nm) due to its very low content in the mixture, high hardness and small original grain size (~ 18 nm) making it difficult to be reduced further. However, the grain size of TiC was decreased from 18 nm to ~ 10 nm and Mo_2C from 31 nm to ~ 20 nm after 60 hrs ball milling.

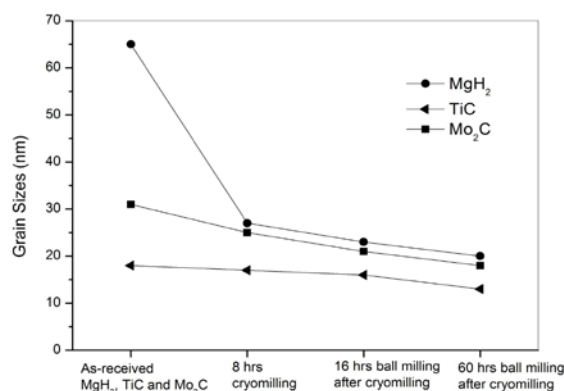


Fig. 2 Grain sizes of MgH_2 , TiC and Mo_2C before and after milling, calculated from XRD patterns of the as-received MgH_2 , TiC , Mo_2C , the ball milled (MgH_2+TiC) and ($\text{MgH}_2+\text{Mo}_2\text{C}$) mixtures

The morphology and microstructure of the mixtures were further investigated by scanning electron microscopy (SEM), shown in Fig. 3. The average particle sizes and the range of particle sizes were calculated according to the SEM images, in Fig. 4. Fig. 3b shows the particle morphology of the as-received TiC , indicating an agglomeration or clustering of nanometer-scaled TiC particles. The as-received Mo_2C consisted of platelet-like particles as shown in Fig. 3c. After 8 hrs cryomilling, the average particle size of the (MgH_2+TiC) is reduced to about ~ 240 nm with irregular morphology (Fig. 3d and Fig. 4), and that of the cryomilled ($\text{MgH}_2+\text{Mo}_2\text{C}$) is ~ 440 nm (Fig. 4). Some of the particles become smaller and others are aggregated to relatively large particles after longer ball milling times of 60 hrs. As shown in Fig. 4, the variation of particle sizes distribution after 60 hrs ball-milling becomes broader compared with that of 8 hrs cryomilling. This is explained by the continuous welding and fracture of particles caused by the collision with milling media balls [24]. The minimum average particles sizes of 60 hrs ball-milled (MgH_2+TiC) and ($\text{MgH}_2+\text{Mo}_2\text{C}$) are 70 nm and 60 nm, respectively, which offers the possibility of inserting them into the grain boundary of MgH_2 . In addition, a smaller particle size or grain size enhances hydrogen absorption/desorption. Because it shortens the hydrogen diffusion path through the bulk area and enlarge grain boundaries and active surface area [25]. From a back-scattered electron (BSE) image of the cryomilled (MgH_2+TiC) (Fig. 3e), the BSE signals for the heavier element or the compound containing heavier element should be observed as much brighter spots. However, the

contrast between the elements of Mg and Ti is not recognized. The distribution of nano-sized TiC particles in the mixture (<100nm) cannot be detected by the SEM-BSE analysis with a resolution in micrometer scale. Whereas from BSE image of 60 hrs ball-milled ($\text{MgH}_2+\text{Mo}_2\text{C}$) after cryomilling (Fig. 3g), small bright particles with 0.1 μm in diameter are uniformly distributed over the larger particles. The bright spots show the distribution of Mo_2C particles because Mg has much smaller atomic number compared with Mo. Mo_2C particles homogeneously distribute in a micrometer-scale range on the surface of MgH_2 .

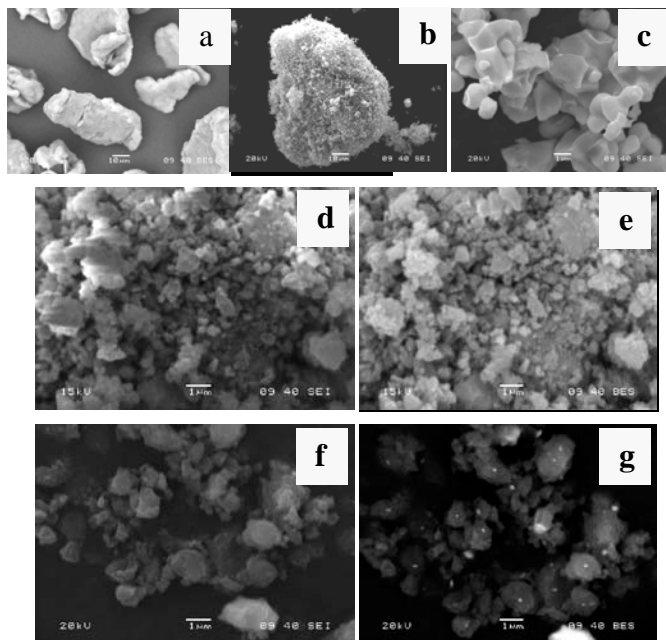


Fig. 3 SEM micrographs of (a) as-received MgH_2 , (b) as-received TiC, (c) as-received Mo_2C , (d) 8 hrs cryomilled (MgH_2+TiC), (e) BSE image of 8 hrs cryomilled (MgH_2+TiC), (f) 60 hrs ball-milled ($\text{MgH}_2+\text{Mo}_2\text{C}$) after cryomilling, and (g) BSE image of 60 hrs ball-milled ($\text{MgH}_2+\text{Mo}_2\text{C}$) after cryomilling

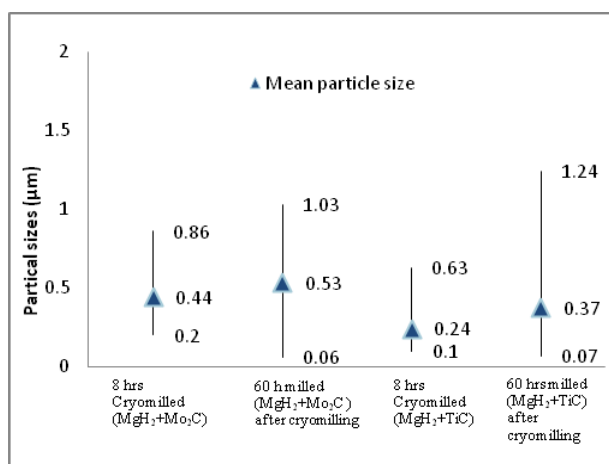


Fig. 4 Mean particle sizes of all samples, calculated from the SEM images of the mixtures

TEM was performed to identify how the TiC particles are distributed in the (MgH_2+TiC) particles on the nanometer scale. Fig. 5 shows the TEM images of the MgH_2 cryomilled for 8hrs and the (MgH_2+TiC) mixture cryomilled for 8 hrs and further ball-milled for 60hrs. The average size of the large particles is estimated to be about 200-400 nm in diameter. There are many much darker small particles decorated on the large particles,

from Fig. 5b. By comparison of Fig. 5a and Fig. 5b, the large bright particles are identified as MgH_2 and the tiny dark particles as TiC. The particle size of TiC is estimated to be 10 ~ 20 nm. From the above observations, the nano-sized TiC particles are either distributed on the surface of MgH_2 particles or inserted between grains of MgH_2 , which enhances the interaction between MgH_2 and TiC. This enhanced interaction explains why TiC acts as an effective catalyst or nucleation site for H_2 sorption, leading to faster kinetics.

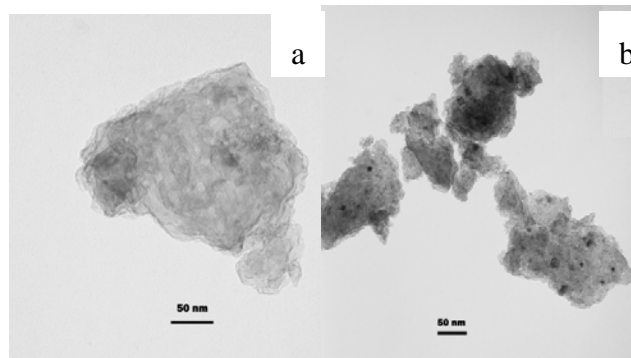


Fig. 5 TEM images of the samples cryomilled for 8 hrs and further ball milled for 60 hrs: (a) MgH_2 and (b) (MgH_2+TiC) mixture

B Hydrogen Desorption Properties

Fig. 6 and Fig. 7 show the thermogravimetric (TG) and derivative thermogravimetric (DTG) curves of hydrogen desorption of the mixtures, respectively. The total relative weight loss of pure MgH_2 , (MgH_2+TiC) and ($\text{MgH}_2+\text{Mo}_2\text{C}$) is, respectively, about 7 wt. %, 6.5 wt. % and 6 wt. %. The 0.5 wt. % and 1 wt. % differences are due to the addition of TiC and Mo_2C . The theoretical capacities of H_2 storage are 7.6 wt. % for pure MgH_2 , 7.3 wt. % for ($\text{MgH}_2+2\text{mol. \%TiC}$) and 6.7 wt. % for ($\text{MgH}_2+2\text{mol. \%Mo}_2\text{C}$). The weight loss between the observed value and the theoretical value of hydrogen releasing is due to the formation of MgO and hydrogen releasing during the long milling time.

DTG curves are calculated to identify the onset and peak temperatures. It is reported that there is good agreement with the decomposition temperature and the peak temperature between DTG and Differential Thermal Analysis (DTA) [26, 27]. This simply means that the maximum rate of weight loss occurs at the greatest temperature differential recorded by DTA [27]. The 8 hrs cryomilled MgH_2 without the catalysts starts to decompose at 320 °C (See Tab. 1). The starting desorption temperature of cryomilled MgH_2 is much lower compared to that of the as-received MgH_2 ($T_{\text{onset}}=418$ °C, $T_{\text{peak}}=434$ °C), which is due to the effect of milling on particle and grain size reduction. With the addition of TiC to the cryomilled sample, the starting temperature of H_2 desorption decreased further to 280°C with a peak temperature of 332 °C. After a further 60 hrs ball-milling of cryomilled (MgH_2+TiC), the onset temperature was reduced to 190°C due to the smaller grain size and enhanced interaction between TiC and MgH_2 . The catalytic effect of TiC is particularly important in reducing the decomposition temperature of MgH_2 , as it has a more pronounced effect upon the starting desorption temperature. For 60 hrs-milled ($\text{MgH}_2+\text{Mo}_2\text{C}$) mixtures, the onset and peak temperature of hydrogen releasing are 300 °C and 358 °C. The addition of Mo_2C does not have an obvious effect on the dehydrogenating temperature. Thus it is believed that TiC for dehydrogenation of MgH_2 has an alternative mechanism of reaction to Mo_2C . Discussion follows.

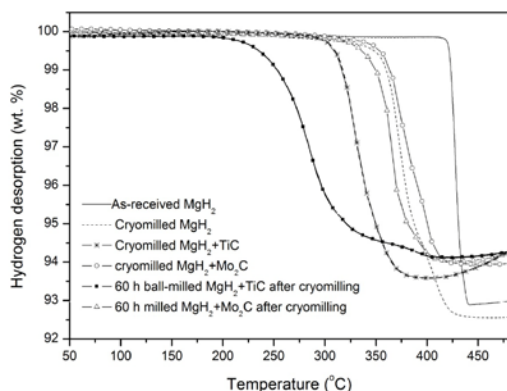


Fig. 6 Thermogravimetric (TG) curves of MgH₂ milled with and without TiC or Mo₂C at the heating rate of 10 K/min under 1 bar He flow

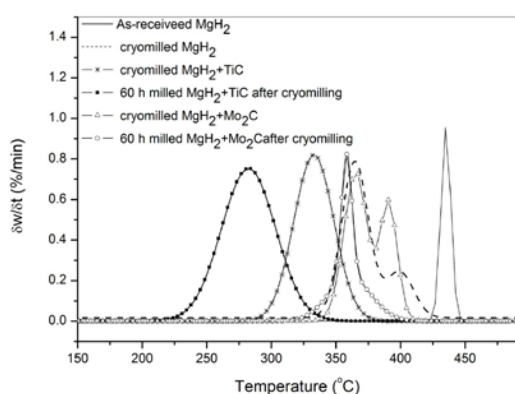


Fig. 7 Derivative thermogravimetric (DTG) curves of MgH₂ milled with and without TiC or Mo₂C at the heating rate of 10 K/min under 1 bar He flow, derived from Fig. 6

The activation energy of the desorption process is estimated by using the following equation:

$$\ln\left(-\frac{dw}{dt}/w\right) = E\left(-\frac{1}{RT}\right) + \ln A \quad (1)$$

Where A is the weight loss of the samples at time t , R is the gas constant (8.314 J/mol/K) and T is the absolute temperature (K), W is the weight fraction remaining. If we assume that the activation energy E is constant over a specific temperature range, then the slope of a plot versus $\left(-\frac{1}{RT}\right)$ over this range

should be equal to the activation energy E [26, 27]. From the slope of the fitted line, the overall activation energy (E') of H₂ desorption of the samples is obtained, as shown in Tab. 1. The activation energy of desorption is as high as 235 kJ/mol for as-received MgH₂. When TiC nanoparticles are added, the value is decreased to 157 kJ/mol after 8 hrs cryomilling. With further ball milling to 60 hrs after cryomilling, the activation energy becomes as low as 104 kJ/mol. Thus desorption kinetics can be improved greatly by high energy milling and catalysis with TiC nanoparticles. The activation energy of (MgH₂ + Mo₂C) ball milled for 60 hrs after cryomilling is 167 kJ/mol. The activation energy of cryomilled MgH₂ and (MgH₂ + Mo₂C) has similar value, 199 kJ/mol and 197 kJ/mol, respectively. Thus Mo₂C does not show catalytic effect on dehydrogenation of MgH₂. The results of activation energy and dehydrogenation

temperature are in correspondence. The desorption kinetics are improved by the addition of Mo₂C and TiC nanoparticles. However, the catalytic effect of TiC is much more pronounced with similar particle size, compared with Mo₂C.

TABLE 1 ONSET & PEAK TEMPERATURE AND DESORPTION RATES FOR THE MgH₂ MILLED TiC OR Mo₂C.

Sample	Onset Temp. (°C) ¹	Peak Temp. (°C) ¹	E' (kJ/mol) ²
As-received MgH ₂	418	434	235
8 hrs cryomilled MgH ₂	330	365	199
8 hrs cryomilled (MgH ₂ + TiC)	280	332	157
60 hrs ball milled (MgH ₂ + TiC) after cryomilling	190	275	104
8 hrs cryomilled (MgH ₂ + Mo ₂ C)	320	360	197
60 hrs ball milled (MgH ₂ + Mo ₂ C) after cryomilling	300	358	167

The phenomenon of mechanical milling helps to pulverize the particles of MgH₂ into nanocrystalline phases and thus leads to lowering the activation energy of desorption [16]. The height of the activation energy barrier depends on the surface elements². Without using the catalysts, the activation energy of H₂ desorption corresponds to the activation barrier for the dissociation of hydrogen atoms from hydrides and the formation of hydrogen molecules. The activation energies of the H₂ desorption for the as-received MgH₂, milled MgH₂ and metal carbide-doped MgH₂, are shown in Tab. 1. On the one hand, the interaction between the H₂ atoms and transition metal carbide particles increases with the particle size decrease of MgH₂ and the catalyst. On the other hand, TiC significantly reduces the energy barrier of dehydrogenation after milling, showing a good catalyst effect than Mo₂C. It has been reported that metallic Ti could catalytically improve the hydrogen storage property of Mg-based hydride. There are two fundamental theories reported for enhancement of the reaction kinetics of MgH₂ with these dopants. One believes the interactions between the hydrides and the Ti-containing agents weaken the Mg-H bonds and favor the recombination of hydrogen atoms toward the hydrogen molecules [7, 10]. Examples include the classic Ti-halides (e.g. TiCl₃) reacting with MgH₂ to form TiH_x, which acts as the catalyst responsible for hydrogen dissociation/recombination at the surface of hydride after ball milling and hydriding/dehydriding processes. The other opinion is that Ti or metallic Ti acts as a classic catalyst for hydrogen dissociation/recombination on the surface of reacting solids [28, 29]. From XRD analysis, both TiC and Mo₂C didn't react with MgH₂ during the milling and dehydriding processes. This means that TiC, Mo₂C and MgH₂ maintain their original phase structures in different hydriding/dehydriding stages throughout, as shown from the XRD patterns in Fig. 1. These results prove that TiC and Mo₂C

¹ Onset and peak temperature of γ -MgH₂

² Activation energy calculated from Eq. 1

nanoparticles exist stably and superlatively around the MgH_2 as the catalytically active species for the reversible hydrogen storage process of the composite.

It is believed that the dehydrogenation of magnesium hydride involves the following steps: decomposition of hydride phase to form magnesium phase, diffusion of hydrogen atoms, and combination with hydrogen atoms into molecules around the TiC or Mo_2C active sites and desorption of hydrogen molecules [28, 30]. Through 8 hrs cryogenic milling and further 60 hrs ball-milling, MgH_2 mixed with the TiC can produce a favorable reactive surface and a large amount of defects acting as active sites for hydrogen and metal interaction. The active sites on catalysts have a stronger ability to absorb hydrogen atoms than MgH_2 , which weaken the bonding of Mg-H. SEM and TEM analysis show that some of TiC nanoparticles have been inserted into the MgH_2 grain boundaries, but Mo_2C particles have relatively large particle size and are only distributed on the surface of MgH_2 . Therefore, the diffusion of hydrogen atoms from bulk area to the surface or grain boundaries is easier and quicker for MgH_2 catalyzed with TiC. From the DTG analysis, the onset and peak temperature of desorption of the (MgH_2 +TiC) is much lower than (MgH_2 + Mo_2C) at the same molar amount and heating rate. Likewise the activation energy of desorption of (MgH_2 +TiC) is much lower than (MgH_2 + Mo_2C). The grain boundary insertion of TiC nanoparticles could be reasons that the catalytic effect of TiC is greater than Mo_2C on hydrogen desorption of MgH_2 . From Fig. 4, there is no big difference in particle size between cryomilled and ball-milled (MgH_2 +TiC). However, the hydrogen desorption properties and kinetics of 60 hrs milled (MgH_2 +TiC) is much better than 8 hrs cryomilled (MgH_2 +TiC). This is because the high energy ball milling for 60 hrs forces some of TiC nanoparticles into the grain boundaries of Mg/ MgH_2 . Consequently, the catalytic effect on the inner phase transformation and growth is improved.

Although it has been reported that the hydrogen storage properties of MgH_2 can be improved effectively by many catalysts, the mechanisms for these catalytic enhancements are still not fully understood. A magnesium-hydrogen reaction mechanism associated with transition metal-based catalysts has been proposed by Barkhordarian et al. [31]. Hydrogen molecules are dissociated mainly on the transition-metal ions of the catalysts, with the formation of a hydrogen-transition-metal bond. Transition metal ions with multiple valence states allow them to dissociate hydrogen molecules and pass hydrogen atoms to the nearby magnesium atoms, where a magnesium hydride is then formed. Therefore the other possibility of the limited effect of Mo_2C on hydrogen desorption of MgH_2 is due to the lower valence state of molybdenum in Mo_2C than titanium in TiC. During desorption, the transition-metal ions of the catalysts form an intermediate state which allows easier recombination of hydrogen atoms toward the molecular state. The affinity of hydrogen to Ti (or the reaction energy of Ti ions with hydrogen) is stronger than that to Mo [32]; hence TiC shows better catalytic properties than Mo_2C in this case.

IV. CONCLUSIONS

The effects of TiC and Mo_2C on hydrogen desorption of MgH_2 by cryomilling and high energy ball milling were investigated and compared. Cryogenic milling is effective in reducing grain sizes and particle sizes. Mo_2C has a limited effect on hydrogen desorption of MgH_2 due to relative large particle sizes and less reduction in activation energy. In

contrast, the addition of TiC substantially reduces desorption temperatures to 190 °C after cryomilling and further high energy ball milling. TiC decreases activation energy of dehydrogenation of MgH_2 from 235 to 104 kJ/mol, representing a good catalytic effect. The insertion of TiC nanoparticles into MgH_2 grain boundary shortens the hydrogen diffusion distance and weakens the bonds of hydrogen and Mg.

ACKNOWLEDGEMENT

This work was supported by the EPSRC (Ref.: EP/E037267/1), which is gratefully acknowledged.

REFERENCES

- [1] M. S. Dresselhaus and I. L. Thomas, Alternative energy technologies, *Nature*, vol. 414, pp. 332-337, 2001.
- [2] Michael U. Niemann, Sessa S. Srinivasan, Ayala R. Phani, Ashok Kumar, D. Yogi Goswami, and Elias K. Stefanakos, Nanomaterials for hydrogen storage applications: a review, *Journal of Nanomaterials*, vol. 2008, 2008.
- [3] L.-P. Ma, P. Wang, and H.-M. Cheng, Hydrogen sorption kinetics of MgH_2 catalyzed with titanium compounds, *International Journal of Hydrogen Energy*, vol. 35, pp. 3046-3050, 2010.
- [4] M. Tian and C. Shang, Nano-structured MgH_2 catalyzed by TiC nanoparticles for hydrogen storage, *Journal of Chemical Technology & Biotechnology*, vol. 86, pp. 69-74, 2011.
- [5] C. X. Shang, M. Bououdina, Y. Song, and Z. X. Guo, Mechanical alloying and electronic simulations of (MgH_2 +M) systems (M=Al, Ti, Fe, Ni, Cu and Nb) for hydrogen storage, *International Journal of Hydrogen Energy*, vol. 29, pp. 73-80, 2004.
- [6] J. H. Shina, G.-J. Leea, Y. W. Chob, and K. S. Lee, Improvement of hydrogen sorption properties of MgH_2 with various sizes and stoichiometric compositions of TiC, *Catalysis Today*, vol. 146, pp. 209-215, 2009.
- [7] X.-D. Kang, P. Wang, and H.-M. Cheng, Advantage of TiF_3 over TiCl_3 as a dopant precursor to improve the thermodynamic property of Na_3AlH_6 , *Scripta Materialia*, vol. 56, pp. 361-364, 2007.
- [8] W. Ping, K. Xiang Dong, and C. Hui Ming, Improved hydrogen storage of TiF_3 -Doped NaAlH_4 , *ChemPhysChem*, vol. 6, pp. 2488-2491, 2005.
- [9] L.-P. Ma, P. Wang, H.-B. Dai, and H.-M. Cheng, Catalytically enhanced dehydrogenation of Li-Mg-N-H hydrogen storage material by transition metal nitrides, *Journal of Alloys and Compounds*, vol. 468, pp. L21-L24, 2009.
- [10] S. Zheng, Fang, J. Zhang, L. Sun, B. He, S. Wei, G. Chen, and D. Sun, Study of the correlation between the stability of Mg-Based hydride and the Ti-Containing agent, *The Journal of Physical Chemistry C*, vol. 111, pp. 14021-14025, 2007.
- [11] J. H. Shin, G.-J. Lee, Y. W. Cho, and K. S. Lee, Improvement of hydrogen sorption properties of MgH_2 with various sizes and stoichiometric compositions of TiC, *Catalysis Today*, vol. 146, pp. 209-215, 2009.
- [12] J. Wang, A. D. Ebner, T. Prozorov, R. Zidan, and J. A. Ritter, Effect of graphite as a co-dopant on the dehydrogenation and hydrogenation kinetics of Ti-doped sodium aluminum hydride, *Journal of Alloys and Compounds*, vol. 395, pp. 252-262, 2005.
- [13] G. Barkhordarian, T. Klassen, and R. Bormann, Catalytic Mechanism of Transition-Metal Compounds on Mg Hydrogen Sorption Reaction, *The Journal of Physical Chemistry B*, vol. 110, pp. 11020-11024, 2006.
- [14] L. Patterson, The Scherrer Formula for X-Ray Particle Size Determination, *Physical Review*, vol. 56, pp. 978-982, 1939.
- [15] R. A. Varin, T. Czujko, and Z. Wronski, Particle size, grain size and γ - MgH_2 effects on the desorption properties of nanocrystalline commercial magnesium hydride processed by controlled mechanical milling, *Nanotechnology*, p. 3856-3865, 2006.
- [16] J. Huot, G. Liang, S. Boily, A. Van Neste, and R. Schulz, Structural study and hydrogen sorption kinetics of ball-milled magnesium hydride, *Journal of Alloys and Compounds*, vol. 293-295, pp. 495-500, 1999.
- [17] F. C. Gennari, F. J. Castro, and G. Urretavizcaya, Hydrogen desorption behavior from magnesium hydrides synthesized by reactive mechanical alloying, *Journal of Alloys and Compounds*, vol. 321, pp. 46-53, 2001.
- [18] M. Bortz, B. Bertheville, and K. Yvon, Structure of the high pressure phase γ - MgH_2 by neutron powder diffraction, *Journal of Alloys and Compounds*, vol. 287, pp. L4-L6, 1999.

- [19] D. L. Vrel, J.-M. Lihmann, and J.-P. Petit, Synthesis of titanium carbide by self-propagating powder reactions. 1. Enthalpy of formation of TiC, *Journal of Chemical & Engineering Data*, vol. 40, pp. 280-282, 1995.
- [20] NASA, NASA polynomials: <http://cea.grc.nasa.gov>, Glenn research center.
- [21] C. Suryanarayana, Mechanical alloying and milling, *Progress in Materials Science*, vol. 46, pp. 1-184, 2001.
- [22] H. J. Fecht, Nanostructure formation by mechanical attrition, *Nanostructured Materials*, vol. 6, pp. 33-42, 1995.
- [23] S. Kalia, Cryogenic Processing: A Study of materials at low temperatures, *Journal of Low Temperature Physics*, pp. 934-945, 2009.
- [24] K. H. Chung, J. He, D. H. Shin, and J. M. Schoenung, Mechanisms of microstructure evolution during cryomilling in the presence of hard particles, *Materials Science and Engineering A*, vol. 356, pp. 23-31, 2003.
- [25] Ranjbar, Z. P. Guo, X. B. Yu, D. Wexler, A. Calka, C. J. Kim, and H. K. Liu, Hydrogen storage properties of MgH₂-SiC composites, *Materials Chemistry and Physics*, vol. 114, pp. 168-172, 2009.
- [26] L. Zhang, J. Ma, X. Zhu, and B. Liang, Kinetics of thermal degradation of thermotropic poly(p-oxybenzoate-co-ethylene-2,6-naphthalate) by single heating rate methods, *Journal of Applied Polymer Science*, vol. 91, pp. 3915-3920, 2004.
- [27] J. H. CHAN and S. T. BALKE, The thermal degradation kinetics of polypropylene: Part III. Thermogravimetric analyses, *Polymer degradation and stability*, vol. 57, pp. 135-149, 1997.
- [28] Kircher and M. Fichtner, Hydrogen exchange kinetics in NaAlH₄ catalyzed in different decomposition states, *Journal of Applied Physics*, vol. 95, pp. 7748-7753, 2004.
- [29] X. Xiao, X. Fan, K. Yu, S. Li, C. Chen, Q. Wang, and L. Chen, Catalytic mechanism of new TiC-doped sodium alanate for hydrogen storage, *The Journal of Physical Chemistry C*, vol. 113, pp. 20745-20751, 2009.
- [30] X. Xu and C. Song, Improving hydrogen storage/release properties of magnesium with nano-sized metal catalysts as measured by tapered element oscillating microbalance, *Applied Catalysis A: General*, vol. 300, pp. 130-138, 2006.
- [31] G. Barkhordarian, T. Klassen, and R. Bormann, Catalytic mechanism of transition-metal compounds on Mg hydrogen sorption reaction, *Journal of Physical Chemistry B*, vol. 110, pp. 11020-11024, 2006.
- [32] P. Atkins, T. Overton, J. Rourke, M. Weller, and F. S. Armstrong, *Atkins inorganic chemistry*, Oxford University Press: Oxford, UK, 2006, pp. 286-289.